Stable EMT type zeolite/CsPbBr 3 perovskite quantum dot nanocomposites for highly sensitive humidity sensors

Xinran Zhang, Jiekai Lv, Jingshi Liu, Shihan Xu, Jiao Sun, Lin Wang, Lin Xu, Svetlana Mintova, Hongwei Song, Biao Dong

Stable EMT type zeolite/$CsPbBr_3$ perovskite quantum dot nanocomposites for highly sensitive humidity sensors

Xinran Zhang[a], Lv Jiekai[a], Jingshi Liu[a], Shihan Xu[d], Jiao Sun[b]*, Lin Wang[c]*, Lin Xu[a], Svetlana Mintova[e], Hongwei Song[a], Biao Dong[a]*

[a]*State Key Laboratory on Integrated Optoelectronics, College of Electronic Science and Engineering, Jilin University, 2699 Qianjin Street, Changchun, 130012, P. R. China.*

[b]*Department of Cell Biology Norman Bethune College of Medicine Jilin University Changchun 130021, China*

[c]*Department of Oral Implantology, School of Dentistry Jilin University, Changchun 130021, China*

[d]*Department of Bioengineering, University of Washington, Seattle, United States.*

[e]*Laboratoire Catalyse et Spectrochimie (LCS), ENSICAEN, Université de Caen, CNRS, 14050 Caen, France*

Keywords:
Humidity sensor, Perovskite, Nano-zeolite, Luminescence mechanism

Abstract

Perovskite quantum dots (PQDs) have been widely studied due to the outstanding light emission properties including high quantum efficiency, narrow linewidths and electron transport properties. However, poor stability limits their implication in optical devices, especially working at ambient conditions in the presence of moisture that rapidly attenuate their performance. In this work, PQDs were loaded in nanosized EMT zeolite crystals synthesized from template-free precursor systems resulting in a composite EMT-$CsPbBr_3$. We found and studied for the first time that, in the pores of the zeolites, a small amount of water molecules can promote the crystallization of perovskite nanocrystals. The energy and bond length of perovskite $CsPbBr_3$ confined in the cages of EMT zeolite were calculated in the presence of water molecules, corresponding to the effect of humidity. Crucially, the pore structure of EMT molecular sieve provides an important research model. The great stability and reliability of the EMT-$CsPbBr_3$ as humidity sensor is presented. The luminous intensity efficiency of the EMT-$CsPbBr_3$ composite was maintained at nearly 90% after continuous usage for 6 months. Both the theoretical and experimental results show that a trace amount of water enhances the luminescence of perovskite stabilized in the hydrophilic EMT zeolite.

1. Introduction

Perovskite quantum dots (PQDs) are becoming an important fluorescent material due to the excellent luminescence properties, including narrow, adjustable emission wavelength, high quantum yield, and low photo bleaching [1-3]. The inorganic PQDs, $CsPbX_3$ (X = Cl, Br, and I), have demonstrated dramatically improved optical performance [4]. The perovskite quantum dots may be considered to replace traditional luminescent materials due to the possible change the wavelength of light by adjusting the proportion of the halogen element and become adaptable for the full visible light spectrum (380 nm - 780 nm) [4-6]. Besides, they have been applied in light emitting diodes [7], solar cell [8] and bioluminescent labeling [9]. However, the low stability of PQDs limits their applications [10]. High ionic conductivity has been reported in the early 1980s, which is considered to be a cause of photoelectric instability of the perovskite materials with a rapid ion exchange in leading halide perovskite nanocrystals (LHP NCs) [10, 11]. Furthermore, the strong ionic character of the PQDs makes it sensitive to polar solvents, which causes formation of surface defects, agglomeration and uncertainty with significant fluorescence quenching. To solve these problems, surface passivation and coating modification of the LHP NCs were considered to improve their stability, such as organic polymers [12, 13] or inorganic materials [14, 15]. Snaith et al. [12] investigated organic-inorganic metal halide perovskites which were blended $CH_3NH_3PbX_3$ PQDs with a desired amount of polystyrene (PS) or polymethyl methacrylate (PMMA). By tailoring the composition of methyl and octlyammonium cations, the perovskite crystal/polymer can prevent the ion exchange and enhance the photoluminescence efficiency. Another organic-inorganic perovskite nanoparticles immobilized in polymer matrixes were reported by Dong et al. [13]. Using the swelling-deswelling microencapsulation, the $MAPbBr_3$-polymer composite films without protection have shown high stability against water. However, most of the polymerization processes involve water, strong polar solvents and other factors that affect the luminous performance. Silica-coating is also commonly used to protect PQDs from water. Zhong et al. [14] prepared $CsPbBr_3@SiO_2$ core-shell nanoparticles (NPs) by one-pot synthesis approach. The green emission of the $CsPbBr_3@SiO_2$ core-shell NPs dispersed in water after 8 minutes increased under ultrasonication in comparison to the uncoated $CsPbBr_3$ nanocrystals (NCs). Other attempts on introducing PQDs into porous SiO_2 and zeolites were also

reported [15]. Microporous zeolites with ion exchange performance can stabilize inorganic metal clusters and protect them from aggregation [16-18]. Ye et al. synthesized a $CsPbX_3$-zeolite-Y composite [16]. After 13 days, the $CsPb(Br_{0.5},I_{0.5})_3$-zeolite-Y composite showed a smaller blueshift of emission (23nm) than bare PQDs without emission reducing. Wang et al. [17] synthesized a composite via encapsulation of perovskite in the AlPO-5 zeolite. Because of exciton confinement and trap passivation, the $MAPbBr_3$@AlPO-5 composite showed efficient radiative emission, and photo-luminescence quantum yield (PLQY) reached 18.2%. The composite immersed in water for more than 2 weeks can emit bright green light under UV illumination.

Till date, the above works indicated that the resistance of the $CsPbX_3$ to water or other polar solvents has been considered the most important issue for photoelectric devices and biological applications, however, the behavior of PQDs in water is not clearly understood yet. The stability issue is their easy degradation in water and even in moisture conditions owing to their ionic nature [15, 18]. Edoardo Moscon et al. presented Ab initio molecular dynamics simulations and according to their calculations, interaction between water molecules and $MAPbI_3$ perovskite surfaces, MAI-terminated surfaces undergo a rapid solvation process with release of I atoms [18]. Therefore, the water vapor causes a significant vacuum-level downshift, and the valence band binding energy referenced to the Fermi level simultaneously increases so as to keep the ionization potential of the perovskite unchanged [19].

It is generally accepted that the PQDs gradually decomposed in high humidity environment, however, how small amounts of water molecules affect perovskite nanocrystals is unclear. In addition, the influence of water molecules on perovskites is not all negative, because the initial water molecules may promote the crystallization of perovskites [20], while it is difficult to find a suitable research model to deeply understand this question, and how to construct a research model with a small amount of water molecules and perovskite is the key to this issue.

In this study, we selected nanosized EMT type ultra-small zeolite nanocrystals ($Na_2O–Al_2O_3–SiO_2–H_2O$) [21] as a host for the PQDs due to the small crystal size and high water capacity. Through the perovskite/zeolite composite, a model for studying the influence of the initial water confined in the pores of zeolites perovskite crystals was created. The crystallization of perovskite nanocrystals confined in EMT zeolites can be detected in real time with different amount of water molecules and theoretical simulation analysis for this model under different

humidity was carried out. What surprised us was that based on the protection of EMT type zeolites, the luminescent performance of perovskite gradually improved when the amount of water molecules increased, and accompanying visible change in sample color, which can be used as a highly sensitive fluorescent probe for humidity detection. Furthermore, the luminescence reversibility of the EMT-$CsPbX_3$ composites at various humidity level was demonstrated. The luminescent intensity of perovskite nanocrystals showed a linear relationship with the humidity increase in the EMT zeolite, which renders the composite as an appropriate material for humidity sensing.

2. Experimental section

2.1 Materials and instruments

Sodium hydroxide (NaOH, reagent grade, 98%, pellets (anhydrous)), sodium silicate (Na_2SiO_3), sodium phosphate dibasic (Na_2HPO_4), sodium aluminate (technical, anhydrous), cyclohexane (AR 99.5%, anhydrous), isopropyl alcohol (AR 99.7%), ethanol (AR 99.7%), potassium hydroxide dehydrate ($KOH·2H_2O$, 85%, pellets), magnesium dichloride hexahydrate ($MgCl_2·6H_2O$, AR 99%), magnesium zinc nitrate tetrahydrate ($Mg(NO_3)_2·4H_2O$, AR 99.0%), sodium chloride (NaCl, AR 99.5%), potassium chloride (KCl, AR 99.5%), potassium nitrate (KNO_3, AR 99.0%) were purchased from Beijing Chemical Industry. Caesium bromide (CsBr), lead dichloride ($PbCl_2$, 99.99%), lead bromide ($PbBr_2$, 99.99%) were all purchased from Macklin. 1-octadecene (ODE, 90%), oleic acid (OA, 90%), oil amine (OAm, 90%) were purchased from Sigma-Aldrich.

Transmission electron microscopy (TEM) images were recorded on a FEI Tecnai G2 S-Twin microscope operated with an acceleration voltage of 200 kV. UV-vis spectra were recorded on a Shimadzu 3100 spectrometer. Fluorescence measurements were carried out by using a fluorescence spectrophotometer SENS-9000.

2.2 Synthesis of EMT-$CsPbX_3$ composite

In addition to the use of related materials and equipment, the procedures for synthesis of EMT-$CsPbX_3$ composite mainly involved three parts as shown below. First, synthesis of EMT-Cs^+

zeolite: The EMT zeolite was synthesized following the procedure described previously [22]. The EMT power sample (1 g) was treated with CsBr aqueous solution with a concentration of 1 mol/L at 60 ^{o}C under the stirring for 6 hours. After the purification (pH=8), the EMT-Cs sample was dried at 80 ^{o}C in the air for 12 hours. Secondly, preparation of PbX_2 (X=Cl, Br, I) solution: 0.188 mmol PbX_2, 5.0 ml ODE, 1.0 ml OA and 1.0 ml OAm were mixed together in a three-neck bottle under the nitrogen and were stirred at 120 ^{o}C for 1 hour until fully dissolved. Then the solution was cooled down to room temperature and sealed to avoid light refrigeration. Finally, synthesis of EMT-$CsPbX_3$ composite: EMT-Cs^+ powder sample (0.5 g) was mixed with 5.0 ml ODE and subjected to heating at 120 ^{o}C for 30 minutes, followed by increasing temperature to 150 ^{o}C. Then the dissolved PbX_2 solution was added, and after 10 minutes the suspension was cooled down to 40 ^{o}C. The sample was further purified with cyclohexane (99.9%) and isopropyl alcohol (99.9%), and subjected to vacuum drying (60 ^{o}C) for 10 hours. At the end, EMT zeolite containing perovskite quantum dots (sample EMT-$CsPbBr_3$) were fabricated and the synthesis process is schematically presented in Fig. 1a. The whole synthesis procedure of each sample is repeatable via strict operation and defined parameters, and the relative standard deviation (RSD) of the measurements for the five sensors was less than 5%, indicating a good reliability.

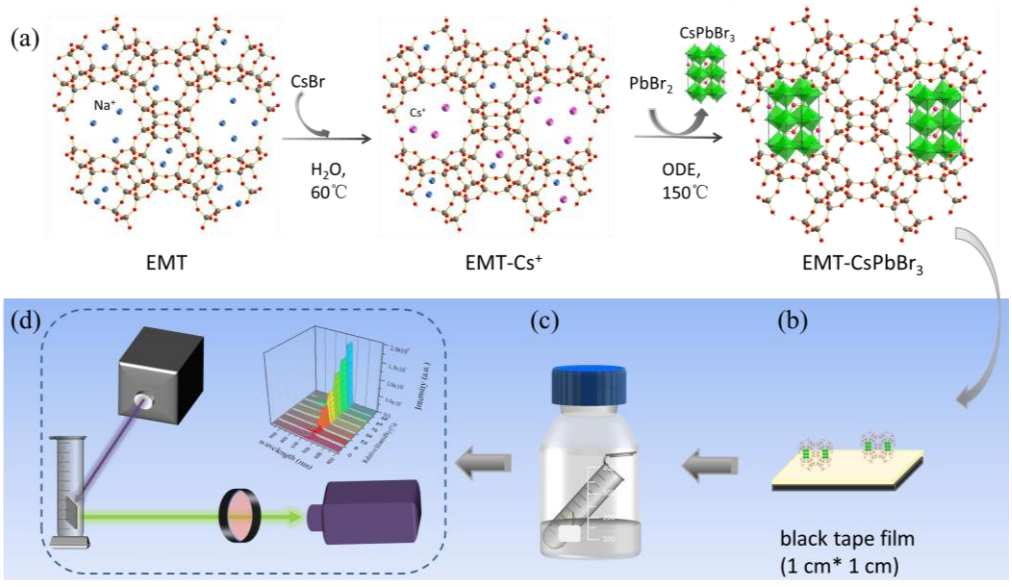

Fig. 1 (a) Synthesis procedure for preparation of EMT-perovskite quantum dots (EMT-$CsPbBr_3$). (b) Deposition of 10 mg EMT-$CsPbBr_3$ sample on a black tape substrate (1cm2), (c) The EMT-CsPbBr3 sample was subjected to different humidity environment (RH=9%, 33%, 53%, 75%, 84% and 92%) for 1 min. (d) Fluorescence spectra recorded from the EMT-$CsPbBr_3$ sample subjected to different RH. diagram for manufacturing 3DIO WO_3/Au films.

2.3 Gas sensors measurements using EMT-$CsPbBr_3$ composite

To clearly explore luminescent properties of EMT-$CsPbBr_3$ on the sensitivity, the sensor device was prepared using a black tape substrate with a size of $1cm^2$; the EMT-$CsPbBr_3$ sample (10 mg) was deposited on the support by brushing and pressing approach. Then the sensor was placed in a 10 ml opened centrifuge tube and subjected to different relative humidity for 1 min. The relative humidity is provided by the atmosphere above the saturated salt solutions [23, 24]. The RH (relative humidity) was set to 9%, 33%, 53%, 75%, 84% and 92% with the corresponding saturated salt solutions of KOH, $MgCl_2$, $Mg(NO_3)_2$, NaCl, KCl, KNO_3, respectively. The 100 ml saturated salt solutions were placed in 500 ml closed glass chambers at 25 ^oC temperature for 24 h. We repeated the experiment with three sensors, and each one has tested twice. The sensors were exposed to different RH, and then subjected to the fluorescence measurements. The samples were annealed at 60 ^oC for 5 minutes prior to the next measurements.

2.4 Simulation of $CsPbBr_3$ in the EMT cages in the presence of H_2O molecules

The simulation was carried out using periodic DFT method in the generalized gradient approximation (GGA) of Perdew. The Burde and Erzerhof (PBE) [25] with the DMol3 module in Material Studio program package was used [26]. All electron calculations were performed with the Double Numerical plus d-functions DND basis set, the convergence threshold was set as 2×10^{-5} eV. In this model, the EMT cage was fixed and saturated with hydrogen.

3. Results and discussion

3.1 Perovskite quantum dots in nanosized EMT zeolite: EMT-$CsPbBr_3$

The crystalline structure of pure EMT and EMT-$CsPbBr_3$ samples was confirmed by XRD analysis (Fig. 2a). The XRD pattern of the EMT-$CsPbBr_3$ contains the characteristic peaks of both the EMT zeolite (JCPDS 46-0566) and the cubic $CsPbBr_3$ PQDs (JCPDS 54-0752). As relative humidity increased from 9% to 92%, the intensity of characteristic peaks for $CsPbBr_3$ also increased (Fig. 2b). The Bragg peaks at 15.18, 30.64, 37.77, and 43.89^o 2Theta corresponding to (hkl) of (100), (200), (211) and (220), respectively have significantly increased, as the relative

humidity increases. The color of the powder also changed in response to relative humidity, as shown in the corresponding illustration. And the intensity of the EMT characteristic peaks changed slightly, which showed that the moisture did not change the properties of EMT zeolite. To further explore, EMT-$CsPbBr_3$ composite and pure EMT zeolite powders were put on the water of quartz cuvettes, respectively, as shown in the inset of Fig.2a. Under a single wavelength excitation at 365 nm, powder of EMT-$CsPbBr_3$ sample showed green emission rapidly when it was treated with water and the powder of pure EMT zeolite didn't. These suggest not only the good stability of the $CsPbBr_3$ PQDs in the EMT zeolite, but also the promotion of the crystallization of perovskite nanocrystals in the presence of water in the zeolite cages.

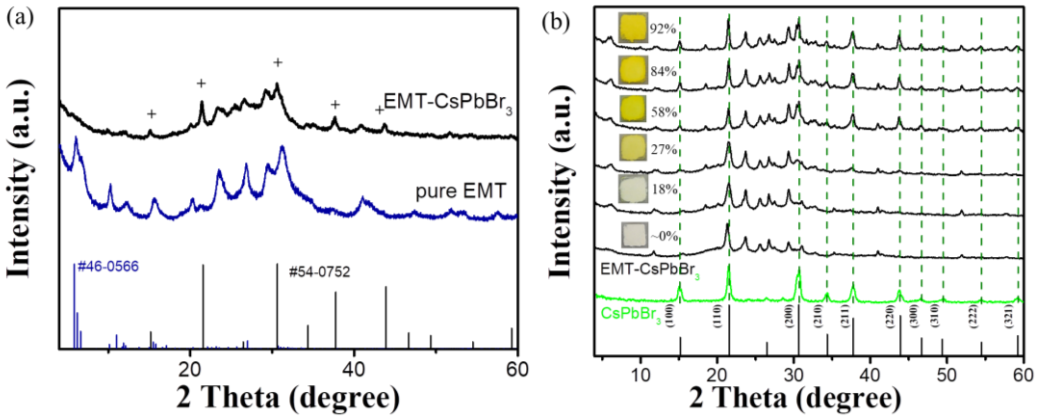

Fig. 2 (a) XRD patterns of pure EMT zeolite, pure $CsPbBr_3$ and (b) perovskite quantum dots stabilized in nanosized EMT zeolite (EMT-$CsPbBr_3$) under different relative humidity (RH= ~0% - 92%). The inset of (a) showed the image of pure EMT zeolite and EMT-$CsPbBr_3$ under UV excitation (365 nm) on the water.

In order to identify the location of the PQDs in the EMT zeolite nanocrystals, HRTEM study of sample EMT-$CsPbBr_3$ was carried out (Fig. 3a, scale bars M = 10 nm). The lattice fringes corresponding to the $CsPbBr_3$ PQDs are shown in Fig. 3b (enlarged red square in Fig. 3a). In Fig. 3b, the lattice fringes with d = 0.52 nm (204) and 0.30 nm (200) coincide well with the crystallographic planes of the EMT zeolite and the cubic $CsPbBr_3$, respectively. The EDS spectrum contains all elements (Na, Si, O, Al, Cs, Pb, Br) thus revealing the existence of Cs, Pb and Br from EMT zeolite; the EDX elemental mapping reveals the distribution of Al, Si, O, Cs, Pb, Br in the same EMT zeolite nanoparticle (Fig. 3 d-j). The $CsPbBr_3$ quantum dots have been successfully divided into the cages of EMT zeolites.

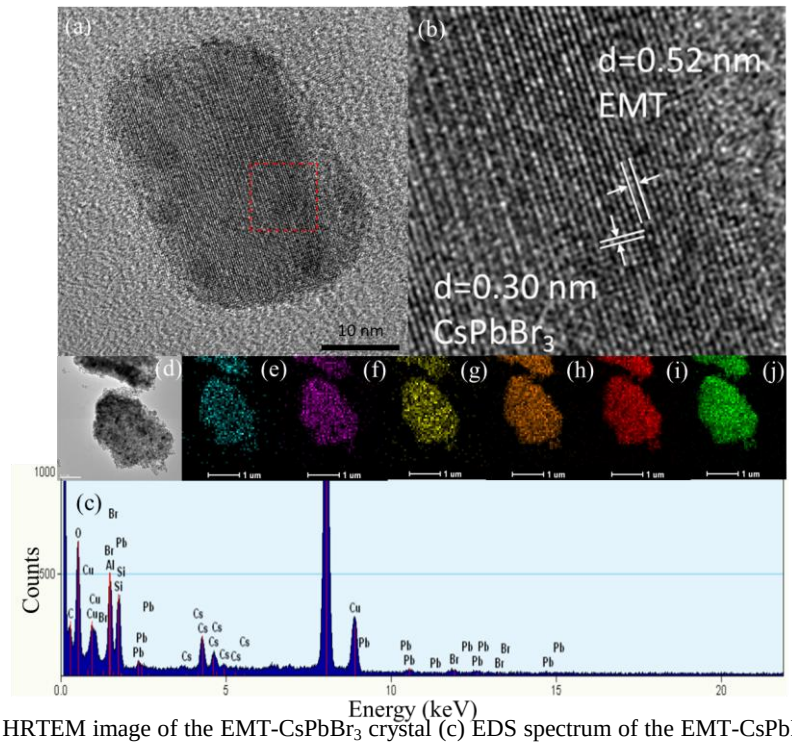

Fig. 3 (a, b) HRTEM image of the EMT-$CsPbBr_3$ crystal (c) EDS spectrum of the EMT-$CsPbBr_3$, (d) TEM picture of EMT-$CsPbBr_3$ crystals subjected to EDS mapping corresponding to (e) Cs, (f) Pb, (g) Br, (h) Si, (i) Al, (j) O.

Further, the EMT-$CsPbBr_3$ sample was characterized by X-ray photoelectron spectroscopy XPS (Fig. 4). The XPS spectra of Cs, Pb, Br, Na, O, Al and Si elements (Fig. S1) conform the incorporation of $CsPbBr_3$ in EMT zeolite nanocrystals. The results confirmed the existence of stable perovskite structure. Fig. 4b shows the binding energy at 138 eV and 143 eV corresponding to Pb $4f_{7/2}$ and Pb $4f_{5/2}$, respectively. The spectra of Cs 3d and Br 3d electrons for $CsPbBr_3$ are presented in Fig. 4c and 4d, respectively [27, 28]. The binding energy of Cs^+ species at 738 eV and 724 eV $3d_{3/2}$ and $3d_{5/2}$ core level are shown in Fig. 4c. The Br with $3d_{3/2}$ and $3d_{5/2}$ binding energy at 68.97 eV and 67.95 eV are clearly seen in Fig. 4d.

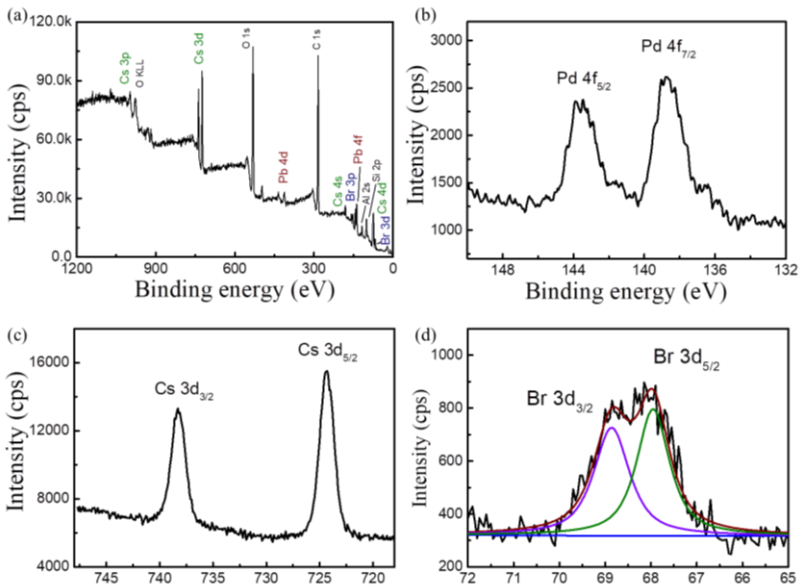

Fig. 4 XPS spectra of the composite corresponding to (a) EMT-$CsPbBr_3$, (b) Pb, (c) Cs and (d) Br.

3.2 Optical properties of EMT-$CsPbBr_3$

In order to analyze the effect of humidity on the PQDs stabilized in the EMT zeolite nanocrystals (Fig. 5a), the emission spectra were measured under excitation at 365 nm. The change of the emission band at 523 nm of the EMT-$CsPbBr_3$ is presented in Fig. 5a. With increasing of the RH%, the luminescent intensity of EMT-$CsPbBr_3$ increased by 16-fold, and the emission peak of $CsPbBr_3$ at 523 nm is linearly enhanced (Fig. 5b). The corresponding fit with the linear equation (y=1978.83*RH(%)-10346.6) (R^2 = 0.9965) and standard error is 50.917. The theoretical limit of detection (LOD) defined as 3S/k (k is the slope of the linear part of the calibration curve and S is the standard deviation of noise in the blank signal) is 0.21% RH presented in Fig. 5b.

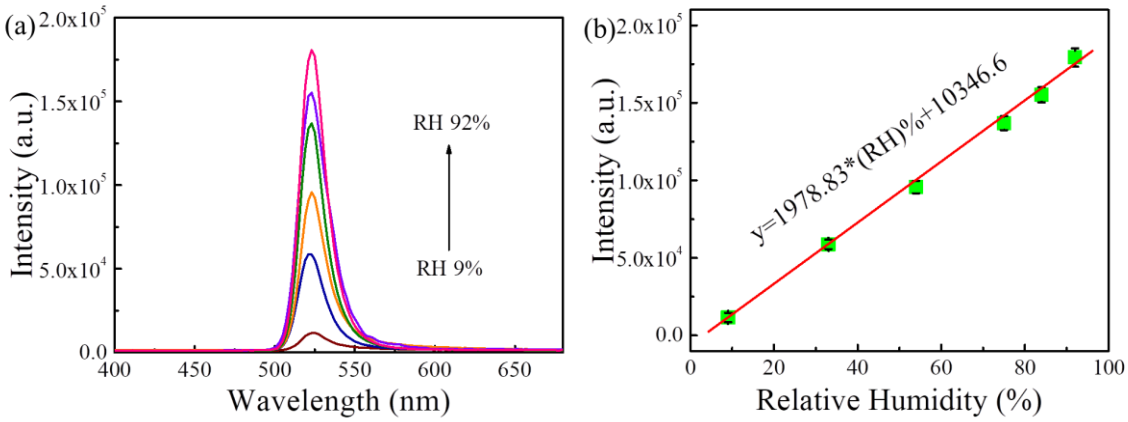

Fig. 5 (a) Emission spectra of perovskite quantum dots in nanosized EMT zeolite (EMT-$CsPbBr_3$) measured at different relative humidity (RH = 9% – 92%) at excitation of 365 nm, and (b) the linear relationship between the RH and luminescent intensity of the EMT-CsPbBr3 under excitation at 365 nm.

The sensitivity and stability of the EMT-$CsPbBr_3$ are higher in comparison to other materials applied as humidity sensors; different materials are summarized in Table 1 [29-33]. These results show that a small increase in the RH% condition has a great effect on the luminescence of the

PQDs stabilized in the EMT nanosized zeolites (EMT-$CsPbBr_3$). And this result is consistent with the increase of the Bragg peaks corresponding to (200) in the XRD patterns (Fig. 2b). When the EMT-$CsPbBr_3$ sample was exposed to human exhalation with high humidity, it will turn yellow within 3 s, indicating a fast response. Compared with common chemical sensors [34, 35], our sensors can work at a lower temperature (25 ^{o}C), which facilitates a wider application. The EMT-$CsPbBr_3$ sensors also showed good selectivity (Fig. S3) and thermal stability (Fig. S4), comparing with other humidity sensors based on inorganic perovskites, because of the protection of EMT zeolite.

Table 1 Summary of the sensing materials, sensing measurements, sensing range, and working temperature.

Sensing Materials	Sensing Measurement	Sensitivity (a.u./RH%)	LOD (RH%)	Sensing Range (RH%)	Stability	Ref.
$CH_3NH_3PbBr_3$	fluorescence	0.1188	0.68	7-98	-	[29]
CdTe/porous silicon	fluorescence	254 (under 50%) 910 (50%-95%)	-	12-93	30 days	[30]
Dye/zeolite	absorbance	2.27×10^{-3}	-	9-92	1 month	[31]
$AlPO_4$-5 zeolite	electrochemical impedance	-	-	11-95	-	[32]
Dye/zeolite	optimal	2.1×10^{-4}	-	6-95	7 days	[33]
EMT-$CsPbBr_3$	fluorescence	1978.83	0.21	0-92	6 months	This work

To further explore the stability, the EMT-$CsPbBr_3$ samples were exposed to different RHs after 1 day and 6 months (treatment at 60 ^{o}C for 2 h to recovery their sensing ability) in Fig. 6. As shown, the characteristic peaks for the $CsPbBr_3$ encapsulated in the EMT nanocrystals enhanced with increasing the RH%, while the Bragg peaks characteristic of EMT retained the same intensity (Fig. 6a). The EMT-$CsPbBr_3$ sample was fully recovered and the performance of the sample was studied after 6 months. As shown in Fig. 6b, the intensity of characteristic peak at 21.4^{o} with (110) for the $CsPbBr_3$ enhanced considerably as the relative humidity increased to 92%, while the other peaks corresponding to the $CsPbBr_3$ decreased. We assume that the long exposure of the sample to water would promote the growth of (200) facets of $CsPbBr_3$. The sample remained nearly 90% of the original luminescent intensity after six months (Fig. 6c), and the corresponding emission spectra were shown in inset of Fig. 6c. However, this situation can only happen in the pore cage of zeolite. In such a small space, only trace amount of water molecules can enter, and the effect of a small amount of water molecules can be realized and observed by the performance of PQDs.

Without the protection of EMT, big amount of water molecules will quickly enter the process of decomposing PQDs.

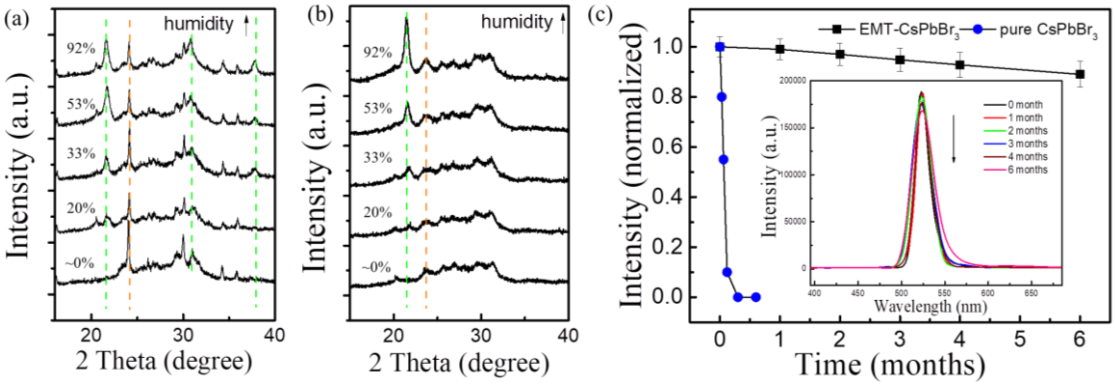

Fig. 6 XRD patterns of the EMT-$CsPbBr_3$ composite after recovery at 60 ^oC: measurements were taken after (a) one day and (b) six months at different relative humidity; (c) luminescent intensity of the EMT-$CsPbBr_3$ and pure $CsPbBr_3$ sample subjected to excitation at 365 nm and RH=92% with the corresponding emission spectra.

3.3 DFT analysis

Accordingly, the perovskite quantum dots stabilized in the nanosized EMT zeolite (EMT-$CsPbBr_3$) showed slow interactions with water. As the relative humidity increased, the EMT zeolites physically adsorbed water leading to stabilization of the perovskite quantum dots.

Before moisture treatment, dry EMT-$CsPbBr_3$ sample showed extremely weak emission peak of $CsPbBr_3$ under excitation at 365 nm. While after exposed to relative humidity environment, water molecules enter through the pores of EMT zeolite, a small amount of water molecules are adsorbed in the cage of EMT, and then trace amount of water molecules enter the inner cage to contact the in-situ grown $CsPbBr_3$ PQDs (as shown in Fig. S5). Before the entry of water molecules, the crystalline conditions of perovskite nanocrystals are poor, leading to weak luminous performance. However, the small amount of water molecules can passivate the defects of the $CsPbBr_3$ PQDs, and promote the growth of Bragg peaks with *hkl* values of (110), (200) and (211) corresponding to the $CsPbBr_3$, therefore, increasing emission was obtained, indicating great sensitivity to water.

To further demonstrate the state of the $CsPbBr_3$ in the EMT zeolite at different RH, we simulate the $CsPbBr_3$ without and with H_2O molecules in the EMT cages.

As we can see in Fig.7a, the $CsPbBr_3$ perovskite lattice is folded before water molecules

entered into the cage of EMT zeolite; the bond angle of 70° for Pb-Br-Pb is calculated, which is unfavorable for crystal growth. In order to understand the influence of water molecules on the perovskite crystal growth in the cages of zeolite, we simulated the situation by adding 1 to 10 water molecules; the bond length and energy of the perovskite nanocrystals were calculated. As the RH% increased, water molecules enter into the cages and tend to combine with -Br to form hydrogen bonds instead of Cs. The perovskite lattice is gradually changed into a straight configuration with an increasing bond angle for Pb-Br-Pb (Fig. 7b-7e), while the angle becomes large again when the number of water molecules is more than six (Fig. 7f-g).

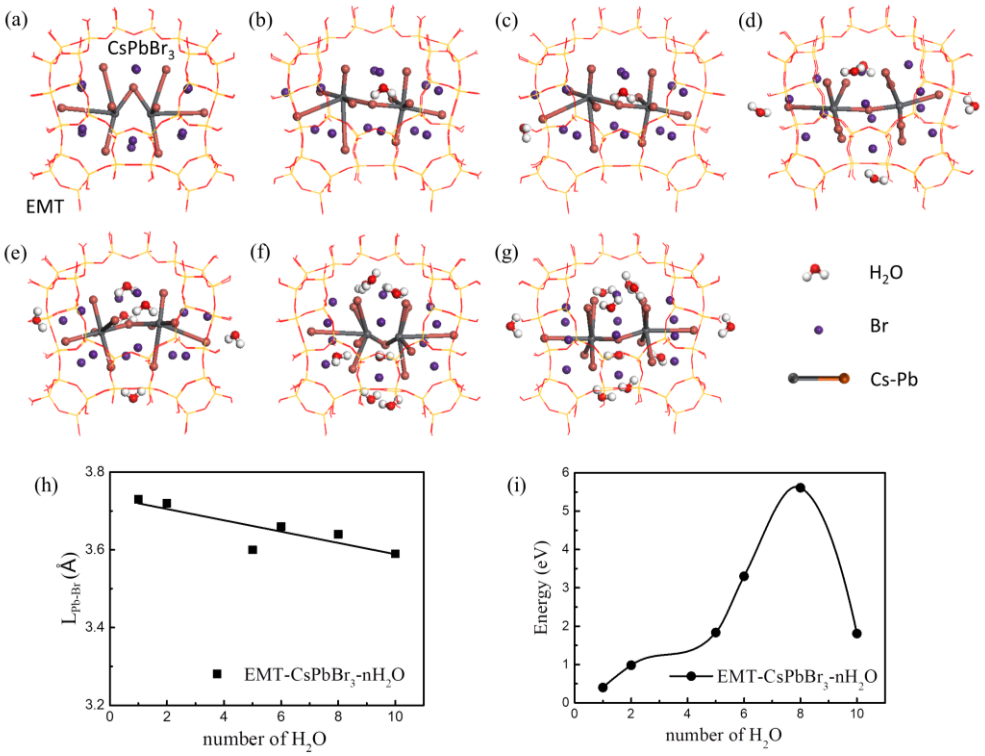

Fig. 7 Main view of perovskite quantum dots ($CsPbBr_3$) (a) without water, and with water (b) $1H_2O$ molecule, (c) $2H_2O$ molecules, (d) $5H_2O$ molecules, (e) $6H_2O$ molecules, (f) $8H_2O$ molecules, and (g) $10H_2O$ molecules in the EMT zeolite cage. (h) Simulated bond lengths LPb-Br of EMT-$CsPbBr_3$ with H_2O in the zeolite cage. (i) The binding energy of EMT-$CsPbBr_3$ with different amount of water molecules.

As the number of water molecules increases from 0 to 10 that combined with $CsPbBr_3$ in EMT zeolite, the average bond length of Pb-Br (L_{Pb-Br}) decreases in general from 3.72Å to 3.58Å, which is closer to 2.93Å in the crystal, as shown in Fig. 7h. Note that the instability of perovskite nanocrystals mainly comes from the dissociation of halogens. Especially when the water content is

high, this reaction will be promoted. But we were surprised to find that in the pores of the EMT zeolite, an appropriate amount of water molecules will enhance the optical property due to the decreased bond length of Pb-Br, showing the improved stability of the perovskite in EMT zeolite.

When $CsPbBr_3$ is combined with 8 H_2O molecules (EMT-$CsPbBr_3$-$8H_2O$), it becomes the most stable with the maximum emission intensity (Table S1). The corresponding trend of change of binding energy of EMT-$CsPbBr_3$-nH_2O is plotted Fig. 7i. These results show that the initial small amount of water will increase the stability of the perovskite, especially in a small enclosed space. The DFT results are consistent with the above experimental data (XRD and optical analysis). This work reports on the highly stable perovskite stabilized in zeolite nanocrystals for applications in solar cell and optoelectronic devices [32].

4. Conclusion

Humidity-sensitive EMT-perovskite quantum dots composites (EMT-$CsPbBr_3$) were synthesized. Note that $CsPbX_3$ PQDs are very sensitive to water, but through the stabilization into EMT zeolite nanocrystals, a significant increase in the stability of perovskite was achieved. The emission of the EMT-$CsPbBr_3$ was enhanced and the color of the sample turns yellow with increasing the moisture content (RH%) and the luminous intensity was fully restored after drying. The reversible performance of the EMT-$CsPbBr_3$ sample was demonstrated after six months, and nearly 90% of the emission intensity was preserved. In our work, it is clear that water molecules have a positive effect on the stability and crystallization of perovskite nanocrystals, which is different from most cases and worthy of further exploration. Note that the pore structure of EMT zeolites can serve as a perfect research model to study the effect of the initial small amount of water molecules on perovskite nanocrystals. By simulating the energy and bond length of perovskite nanocrystals stabilized in the cages of EMT nanozeolite, we found that the dissociation of Br is suppressed, and the overall stability is increased by increasing the amount of water, indicating that an appropriate trace amount of water helps to form PQDs, and enhances the luminescence of perovskite stabilized in the hydrophilic EMT zeolite. Therefore, it is an in-depth understanding of the role and function of water in perovskite materials. Due to the great stability and reliability, EMT-CsPbBr3 based humidity sensor has been achieved with remarkable

performance.

Conflicts of interest

The authors declare no competing financial interest.

Acknowledgments

This work was supported by the National Natural Science Foundation of China (Grant Nos. 52050077, 11874181, 82170998), Major Basic Research Projects of Shandong Natural Science Foundation (ZR2020ZD36), General program of Natural Science Foundation of Jilin Province (20210401059YY, 20200201356JC, 20200201317JC).

References

[1] Akkerman Q A, Rainò G, Kovalenko M V, et al. Genesis, challenges and opportunities for colloidal lead halide perovskite nanocrystals[J]. Nature Materials, 2018.
[2] Alivisatos A P. Semiconductor Clusters, Nanocrystals, and Quantum Dots[J]. Science, 1996, 271(5251):933-937.
[3] Larson D. Water-soluble quantum dots for multiphoton fluorescence imaging in vivo.[J]. Science, 2003, 300(5624):1434-6.
[4] Song J, Li J, Li X, et al. Quantum Dot Light-Emitting Diodes Based on Inorganic Perovskite Cesium Lead Halides ($CsPbX_3$).[J]. Advanced Materials, 2016, 27(44):7162-7167.
[5] Wang Y , Li X , Song J , et al. All-Inorganic Colloidal Perovskite Quantum Dots: A New Class of Lasing Materials with Favorable Characteristics[J]. Advanced Materials, 2015, 27(44):7101-8.
[6] Akihiro K, Kenjiro T, Yasuo S, et al. Organometal halide perovskites as visible-light sensitizers for photovoltaic cells[J]. Journal of the American Chemical Society, 2009, 131(17):6050-6051.
[7] Li J, Xu L, Wang T, et al. 50- Fold EQE Improvement up to 6.27% of Solution- Processed All- Inorganic Perovskite $CsPbBr_3$ QLEDs via Surface Ligand Density Control[J]. Advanced Materials, 2017, 29(5).
[8] Cong Chen, Hao Li, et al. Long-Lasting Nanophosphors Applied to UV-Resistant and Energy Storage Perovskite Solar Cells[J]. Advanced Energy Materials, 2017, 7(20).
[9] Chen X, Li D, Pan G, et al. All-inorganic Perovskite Quantum Dots/TiO_2 Inverse Opal Electrode Platform: A Stable and Efficient Photoelectrochemical Sensing for Dopamine under Visible Irradiation[J]. Nanoscale, 2018:10.1039.C8NR02115E.
[10] A. Swarnkar, A. R. Marshall, E. M. Sanehira, B. D. Chernomordik, D. T. Moore, J. A. Christians, T. Chakrabarti, J. M. Luther, Quantum dot–induced phase stabilization of α-CsPbI3 perovskite for high-efficiency photovoltaics. Science 2016, 354, 92.
[11] Mizusaki J , Arai K , Fueki K . Ionic conduction of the perovskite-type halides[J]. Solid State

Ionics, 1983, 11(3):203-211.
[12] Pathak S, Sakai N, Rivarola F W R, et al. Perovskite Crystals for Tunable White Light Emission[J]. Chemistry of Materials, 2015, 27(23).
[13] Yanan Wang, Juan He, Hao Chen, et al. Ultrastable, Highly Luminescent Organic-Inorganic Perovskite-Polymer Composite Films[J]. Advanced Materials, 2016.
[14] Qixuan Z, Muhan C, Huicheng H, et al. One-Pot Synthesis of Highly Stable CsPbBr3@SiO2 Core-Shell Nanoparticles[J]. Acs Nano, 2018:acsnano.8b04209.
[15] Wei, Ziyong, Cheng,et al. Correction: An overview on enhancing the stability of lead halide perovskite quantum dots and their applications in phosphor-converted LEDs. CHEMICAL SOCIETY REVIEWS, 2018.
[16] Sun J Y, Rabouw F T, Yang X F, et al. Facile Two‐Step Synthesis of All‐Inorganic Perovskite $CsPbX_3$ (X = Cl, Br, and I) Zeolite‐Y Composite Phosphors for Potential Backlight Display Application [J]. Advanced Functional Materials, 2017, 27(45):1704371.
[17] Wang P, Wang B, Liu Y, et al. Ultrastable perovskite‐zeolite composite enabled by encapsulation and in situ passivation[J]. Angewandte Chemie, 2020.
[18]Mosconi E , Azpiroz J M , Angelis F D . Ab Initio Molecular Dynamics Simulations of Methylammonium Lead Iodide Perovskite Degradation by Water[J]. Chemistry of Materials, 2015.
[19] Swarnkar, Abhishek, Marshall, et al. Quantum Dot-Induced Phase Stabilization of. alpha. -$CsPbI_3$ Perovskite for High-Efficiency Photovoltaics[J]. Science, 2016, 354(6308):92.
[20] Liu K K, Liu Q, Yang D W, et al. Water-induced MAPbBr3@PbBr(OH) with enhanced luminescence and stability[J]. Light: Science & Applications, 2020, 9(1):44.
[21] E.P. Ng, D. Chateigner, T. Bein, V. Valtchev, S. Mintova, Capturing Ultrasmall EMT Zeolite from Template-Free Systems, Science, 335(2012) 70-3.
[22] Label-free electrochemical immunosensor based on conductive Ag contained EMT-style nano-zeolites and the application for α-fetoprotein detection, Sensors and Actuators B: Chemical, 2018, 255(3):2919-2926
[23] Greenspan L . Humidity fixed points of binary saturated aqueous solutions[J]. J.res.national Bur.stnd, 1977, 81(1):81--89.
[24] Liu, Wei; A highly sensitive and moisture-resistant gas sensor for diabetes diagnosis with Pt@In2O3 nanowires and a molecular sieve for protection[J]. Npg Asia Materials, 2018.
[25] John, P, Perdew, et al. Generalized Gradient Approximation Made Simple [Phys. Rev. Lett. 77, 3865 (1996)][J]. Physical Review Letters, 1997.
[26] Delley, B. From molecules to solids with the DMol3 approach. J. Chem. Phys. 2000, 113, 7756–7764.
[27] Xiaoming, Li, Ye, et al. Quantum Dots: CsPbX3Quantum Dots for Lighting and Displays: Room-Temperature Synthesis, Photoluminescence Superiorities, Underlying Origins and White Light-Emitting Diodes (Adv. Funct. Mater. 15/2016)[J]. Advanced Functional Materials, 2016, 26(15):2584-2584.
[28] Sun S , D Yuan, Xu Y , et al. Ligand-Mediated Synthesis of Shape-Controlled Cesium Lead Halide Perovskite Nanocrystals via Reprecipitation Process at Room Temperature[J]. Acs Nano, 2016:3648.
[29] Xu W , Li F , Cai Z , et al. An ultrasensitive and reversible fluorescence sensor of humidity using perovskite CH3NH3PbBr3[J]. Journal of Materials Chemistry C, 2016, 4(41):9651-9655.

[30] M.A. Zanjanchi, S. Sohrabnezhad, Evaluation of methylene blue incorporated in zeolite for construction of an optical humidity sensor, Sens. Actuators B 105 (2005) 502–507.

[31] Chen M , Xue S , Liu L , et al. A Highly Stable Optical Humidity Sensors Based on Nano-composite Film[J]. Sensors and Actuators B Chemical, 2019, 287(MAY):329-337.

[32] Gao, Fengli, Zhang. Humidity sensor based on AlPO4-5 zeolite with high responsivity and its sensing mechanism[J]. Sensors and Actuators, B. Chemical, 2015.

[33] Sohrabnezhad S, Pourahmad A, Sadjadi M A. New methylene blue incorporated in mordenite zeolite as humidity sensor material [J]. Materials Letters, 2007, 61(11-12):2311-2314.

[34] Naderi H , Hajati S , Ghaedi M , et al. Sensitive, selective and rapid ammonia-sensing by gold nanoparticle-sensitized V2O5/CuWO4 heterojunctions for exhaled breath analysis[J]. Applied Surface Science, 2019, 501.

[35] Ranjbar F , Hajati S , Ghaedi M , et al. Highly selective MXene/V2O5/CuWO4-based ultra-sensitive room temperature ammonia sensor[J]. Journal of Hazardous Materials, 2021, 416(24).